Proceedings of the Second Asian Conference on Mechanics of Functional Materials and Structures
October 22-25, 2010, Nanjing, China

ANTIPLANE SINGULAR ELECTROELASITC FIELDS OF PIEZOELECTRIC INCLUSION CORNER

Xue-cheng Ping[1], Meng-cheng Chen[2], Nao-Aki Noda[3]

[1,2] *Key Laboratory of Conveyance and Equipment of Ministry of Education*
East China Jiaotong University, Nanchang, CHINA 330013
[3] *Department of Mechanical Engineering, Kyushu Institute of Technology, Kitakyushu, Japan 804-8550*

The aim of current research is to develop an ad hoc hybrid-stress finite element method to solve singular antiplane electroelastic fields in piezoelectric inclusion corner configurations. At first, a super corner tip element is developed based on the variational principles for the corner tip domain together with the numerical eigensolutions of the singular antiplane electroelastic fields. Then, an ad hoc finite element model for the whole piezoelectric domain is established by incorporating the super corner tip element into conventional elements. As application, a rectangular piezoelectric inclusion embedded in another piezoelectric matrix is considered, and the effects of material properties, inclusion sizes and interface delamination on generalized stress and electric displacement intensity factors (GSIFs) are investigated.

Keywords: *piezoelectric, inclusion, corner tip, antiplane, singular electroelastic field*

1 Introduction

Piezoelectric materials are widely used in various fields such as transducers, wave filters, sensors, resonators and actuators. Fully bonded structures are unavoidable. Because of the mismatches of material properties and geometries, the stresses and electric displacements at inclusion corner tips may be discontinuous, and delamination and cracking failures usually initiate at these locations. Because inplane electric fields and antiplane stress fields of piezoelectric materials are often coupled, thus antiplane problems of piezoelectric materials are more complicated than those of common composites. Some traditional analytical methods that have been successfully used for inplane problems of piezoelectric materials, such as complex potential method, distributed dislocation method and integral equation methods are also suitable for antiplane problems [1-4]. On the other hand, numerical method such as the conventional finite element method and the Treffiz finite element method [5] are also be used to deal with antiplane problems. It should be pointed out that the aforementioned methods are only limited to crack or interface crack problems. Recently, a finite element eigen-analysis method [6] and a Mellin transform method [7] are used respectively to solve the eigensolutions of antiplane singular electroelastic fields near the vertex of bonded piezoelectric wedges and junctions. Obviously, the singular stress fields near the vertex of multi-material wedges and junctions depend on not only the eigensolutions but also the GSIFs. In an effort to determine the GSIFs of inplane singular elastic fields, Chen and Ping [8] deal with the inplane problems of inclusion corners in elastic media by a novel hybrid-stress finite element method. In this paper, a hybrid-stress finite element method for the analysis of antiplane singular electroelastic fields of inclusion corners in piezoelectric materials will be deduced.

2 Solution Method

As illustrated in Figure 1, an inclusion corner tip domain composed of bi-piezoelectric material sectors can be partitioned into inner and outer regions. In the inner region of either a closed or open junction, the presence of a singular electroelastic field near the junction arising from the material and geometric discontinuities requires an exact solution of the governing equations. The solution to the outer region in which a singular electroelastic field does exist can be constructed by employing the finite element method with conventional elements. Therefore, an accurate solution to the entire domain requires coupling of the exact solution in the inner region with that of the approximate solution through the finite element method in the outer region. The coupling can be achieved by developing a super corner tip element whose interpolation functions satisfy the governing equations

[1] Associate Professor, xuecheng_ping@yahoo.com.cn
[2] Professor, chenmch@ecjtu.jx.cn
[3] Professor, noda@mech.kyutech.ac.jp

exactly near the junction while enforcing the inter-element displacement and electric potential continuities along the common boundary and the nodes between the corner tip elements and the conventional elements.

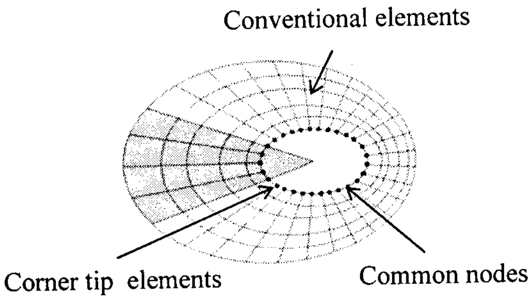

Figure 1: Conventional elements coupled with a global element for a closed junction.

3 Stiffness matrix of the global inclusion corner tip element

To formulate finite element calculations for the antiplane singular electroelastic fields around an inclusion corner-tip in piezoelectric materials, a super *n*-sided polygonal inclusion corner-tip element which contains a part of an inclusion corner, as shown in Figure 2, will be developed based on the computed numerical eigensolutions in Chen and Ping [6].

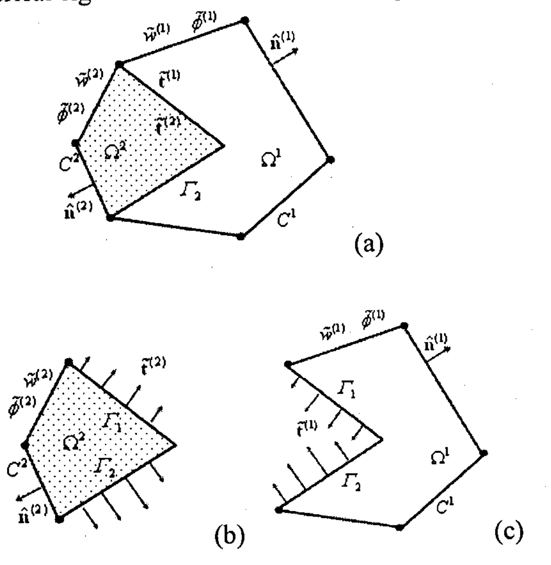

Figure 2: Element decomposition: (a) original element; (b) inclusion domain with mixed boundary values; (c) matrix domain with mixed boundary values

Our goal is to establish the relationship between the element's generalized nodal force and displacement, or simply, to formulate the element stiffness matrix. The key idea in formulating this corner tip element is to decompose the original problem into two boundary value problems as shown in Figures 2(b) and (c): (1) a specified mixed boundary value problem in the matrix domain Ω^1 with boundaries C^1, Γ_1 and Γ_2; (2) a specified mixed boundary value problem in the non-ellipsoidal inclusion domain Ω^2 with boundaries C^2, Γ_1 and Γ_2. C^1 and C^2 are the element's outer boundary with neighboring elements, and Γ_1 and Γ_2 are inner interfaces between the matrix and the inclusion. Following the Hellinger-Reissner principle, we define the following hybrid functional for problem (1):

$$\pi_m^e = \int_{\Omega^1} \Big(\frac{1}{2}\begin{Bmatrix}\boldsymbol{\tau}_m\\ \mathbf{D}_m\end{Bmatrix}^T \mathbf{S}_m \begin{Bmatrix}\boldsymbol{\tau}_m\\ \mathbf{D}_m\end{Bmatrix} - \begin{Bmatrix}\boldsymbol{\tau}_m\\ \mathbf{D}_m\end{Bmatrix}^T \nabla \begin{Bmatrix}w_m\\ \phi_m\end{Bmatrix}\Big) d\Omega - \int_{C^1} (\mathbf{t}_m)^T \Big(\begin{Bmatrix}\tilde{w}^{(1)}\\ \tilde{\phi}^{(1)}\end{Bmatrix} - \begin{Bmatrix}w_m\\ \phi_m\end{Bmatrix}\Big) dS + \int_{\Gamma_1+\Gamma_2} (\tilde{\mathbf{t}}^{(1)})^T \begin{Bmatrix}w_m\\ \phi_m\end{Bmatrix} dS \qquad (1)$$

where w, ϕ, $\boldsymbol{\tau}$, D, $\mathbf{t}$ and $\mathbf{S}$ are, respectively, the displacement, electric potential, stress, electric displacement, generalized boundary traction vectors and the electroelastic compliance matrix; ∇ is the matrix differential operator relating strains and electric fields to displacements and electric potential; the symbol "~" represents a specified quantity. Based on the hybrid-stress finite element method; the subscript "m" denotes components in domain Ω^1; the boundary displacement $\tilde{w}^{(1)}$ and electric potential $\tilde{\phi}^{(1)}$ are assumed separately from w and ϕ and are expressed in terms of the displacements and electric potentials of the element; and the generalized boundary tractions $\tilde{\mathbf{t}}^{(1)}$ is assumed to be specified and are actually unknown.

The stationary values of the functional defined by Eq. (1) yields the following a set of equations:

$$\nabla^T \begin{Bmatrix}\boldsymbol{\tau}_m\\ \mathbf{D}_m\end{Bmatrix} = 0, \quad \mathbf{S}_m \begin{Bmatrix}\boldsymbol{\tau}_m\\ \mathbf{D}_m\end{Bmatrix} = \nabla \begin{Bmatrix}w_m\\ \phi_m\end{Bmatrix} \text{ in } \Omega^1 \qquad (3)$$

$$\mathbf{t}_m = \mathbf{n}^{(1)} \begin{Bmatrix}\boldsymbol{\tau}_m\\ \mathbf{D}_m\end{Bmatrix} \text{ on } C^1,\ \Gamma_1 \text{ and } \Gamma_2 \qquad (4)$$

$$\begin{Bmatrix}w\\ \phi\end{Bmatrix} = \begin{Bmatrix}\tilde{w}^{(1)}\\ \tilde{\phi}^{(1)}\end{Bmatrix} \text{ on } C^1,\ \mathbf{t} = \tilde{\mathbf{t}}^{(1)} \text{ on } \Gamma_1 \text{ and } \Gamma_2 \qquad (5)$$

in which $\mathbf{n}^{(1)}$ is a 3×5 matrix of the unit normal to boundary $C^{(1)}$ and $\Gamma_{(1)}$.

It is seen from the above equations that the true solution of the problem (1) minimizes the hybrid functional. We may simplify the functional by constructing the electroelastic field in such a manner that Eqs. (3) and (4) are automatically satisfied. By doing this and using the divergence theorem over Ω^1, the functional π_m^e is reduced to

$$\pi_m^e = \frac{1}{2}\int_{C^1} \mathbf{t}_m^T \begin{Bmatrix}w_m\\ \phi_m\end{Bmatrix} dS - \int_{C^1} \mathbf{t}_m^T \begin{Bmatrix}\tilde{w}^{(1)}\\ \tilde{\phi}^{(1)}\end{Bmatrix} dS + \int_{\Gamma_1+\Gamma_2} (\tilde{\mathbf{t}}^{(1)})^T \begin{Bmatrix}w_m\\ \phi_m\end{Bmatrix} dS - \frac{1}{2}\int_{\Gamma_1+\Gamma_2} \mathbf{t}_m^T \begin{Bmatrix}w_m\\ \phi_m\end{Bmatrix} dS \qquad (6)$$

In the same way as problem (1), the functional π_{I}^{e} in domain Ω^2 for problem (2) can also be obtained, in which the subscript "I" denotes a functional in domain Ω^2.

In order to recover the solution for the original problem from those of two decomposed problems, the traction reciprocity t conditions and the displacement and electric potential compatibility conditions are necessary to be imposed:

$$\begin{Bmatrix} w_{\mathrm{I}} \\ \phi_{\mathrm{I}} \end{Bmatrix} = \begin{Bmatrix} w_{\mathrm{m}} \\ \phi_{\mathrm{m}} \end{Bmatrix} \text{ on } \Gamma_1 \text{ and } \Gamma_2 \tag{7}$$

$$\mathbf{t}^{(1)} = -\mathbf{t}^{(2)},\ \mathbf{t}_{\mathrm{m}} = -\mathbf{t}_{\mathrm{I}} \text{ on } \Gamma_1 \text{ and } \Gamma_2 \tag{8}$$

The functional π^e for the original problem is rewritten as $\pi^e = \pi_{\mathrm{m}}^e + \pi_{\mathrm{I}}^e$. Therefore, adding Eqs. (5) and (6), and noting conditions (7) and (8), we have

$$\pi^e = \frac{1}{2}\int_C \mathbf{t}^{\mathrm{T}} \begin{Bmatrix} w \\ \phi \end{Bmatrix} \mathrm{d}S - \int_C \mathbf{t}^{\mathrm{T}} \begin{Bmatrix} \tilde{w} \\ \tilde{\phi} \end{Bmatrix} \mathrm{d}S \tag{9}$$

where $C = C^{(1)} + C^{(2)}$.

w, ϕ, $\boldsymbol{\tau}$ and D near the inclusion corner tip can be expressed in terms of asymptotic expressions, i.e.,

$$\begin{Bmatrix} w^e \\ \phi^e \end{Bmatrix} = \mathbf{U}_{\mathrm{C}}^e \boldsymbol{\beta},\ \begin{Bmatrix} \boldsymbol{\tau}^e \\ \mathbf{D}^e \end{Bmatrix} = \boldsymbol{\Sigma}_{\mathrm{C}}^e \boldsymbol{\beta} \tag{10, 11}$$

in which the quantity with subscript C is a new interim one in the Cartesian coordinate system, $\mathbf{U}_{\mathrm{C}}^e$ and $\boldsymbol{\Sigma}_{\mathrm{C}}^e$ are matrices derived from the eigensolutions of singular electroelastic fields[6], and $\boldsymbol{\beta}$ are coefficients to be determined.

The boundary value $\tilde{w}$ of the corner-tip element in Eq. (10) can be expressed with the nodal displacement $\tilde{W}_{\mathrm{C}}^e$ and electric potential $\tilde{\Phi}_{\mathrm{c}}^e$ as

$$\begin{Bmatrix} \tilde{w}^e \\ \tilde{\phi}^e \end{Bmatrix} = \mathbf{L}[\tilde{W}_{\mathrm{C}i}^e, \tilde{\Phi}_{\mathrm{C}i}^e, \tilde{W}_{\mathrm{C}i+1}^e, \tilde{\Phi}_{\mathrm{C}i+1}^e]^{\mathrm{T}} = \mathbf{L}\begin{Bmatrix} \tilde{\mathbf{W}}_{\mathrm{C}}^e \\ \tilde{\boldsymbol{\Phi}}_{\mathrm{C}}^e \end{Bmatrix} \tag{12}$$

where $\mathbf{L}$ is a one-dimensional Lagrangian interpolation function matrix defined on the element boundaries excluding the interfaces between the matrix and the inclusion. Along the boundary segment, the displacement is assumed to be linear, so the interpolation function matrix $\mathbf{L}$ between two adjacent nodes can be expressed as

$$\mathbf{L} = \left[(1-\frac{s}{l})\mathbf{I}_2 \quad \frac{s}{l}\mathbf{I}_2 \right] \tag{13}$$

By substituting Eqs.(10), (11) and (12) into Eq.(9) yields an equation of the form

$$\pi^e = \frac{1}{2}\boldsymbol{\beta}^{\mathrm{T}}\mathbf{H}^e\boldsymbol{\beta} - \boldsymbol{\beta}^{\mathrm{T}}\mathbf{G}^e \begin{Bmatrix} \tilde{\mathbf{W}}_{\mathrm{C}}^e \\ \tilde{\boldsymbol{\Phi}}_{\mathrm{C}}^e \end{Bmatrix} \tag{14}$$

herein

$$\mathbf{H}^e = \frac{1}{2}\int_C \left[\left(\mathbf{n}^e\boldsymbol{\Sigma}_{\mathrm{C}}^e\right)^{\mathrm{T}} \mathbf{U}_{\mathrm{C}}^e + \left(\mathbf{U}_{\mathrm{C}}^e\right)^{\mathrm{T}} \left(\mathbf{n}^e\boldsymbol{\Sigma}_{\mathrm{C}}^e\right) \right] \mathrm{d}S,$$

$$\mathbf{G}^e = \int_C \left[\left(\mathbf{n}^e\Sigma_{\mathrm{C}}^e\right)^{\mathrm{T}} \mathbf{L} \right] \mathrm{d}S,$$

According to the stationary condition of the functional π^e with respect to $\boldsymbol{\beta}$, the functional π^e is expressed in terms of the nodal displacement $\tilde{\mathbf{W}}_{\mathrm{C}}^e$ and electric potential $\tilde{\boldsymbol{\Phi}}_{\mathrm{C}}^e$ only, i.e.,

$$\pi^e = \frac{1}{2}\begin{Bmatrix} \tilde{\mathbf{W}}_{\mathrm{C}}^e \\ \tilde{\boldsymbol{\Phi}}_{\mathrm{C}}^e \end{Bmatrix}^{\mathrm{T}} \left[\mathbf{K}_{\mathrm{inc}}\right]^e \begin{Bmatrix} \tilde{\mathbf{W}}_{\mathrm{C}}^e \\ \tilde{\boldsymbol{\Phi}}_{\mathrm{C}}^e \end{Bmatrix} \tag{15}$$

where the stiffness matrix of the super inclusion corner-tip element is

$$\left[\mathbf{K}_{\mathrm{inc}}\right]^e = (\mathbf{G}^e)^{\mathrm{T}}(\mathbf{H}^e)^{-1}\mathbf{G}^e \tag{16}$$

4 Numerical examples

As shown in Figure 3, an infinite piezoelectric plate including a rectangular piezoelectric inclusion whose length and width are measured as 2L and 2B, respectively, are considered. Poling directions of both materials are oriented in the *z*-axis. Antiplane shear stress τ_z^∞ and inplane electric displacement D_y^∞ are applied to the upper and lower edges of the plate. Due to symmetry of the geometry and loading, only the upper right quarter of the geometry is needed for finite element mesh division. In order to determine the antiplane singular electroelastic fields near the point o_1, an 8-node super inclusion corner tip element is used around this point.

When singular stresses at every polar angle θ are calculated, the GSIFs can also be obtained, i.e.,

$$\mathrm{K}_1 = \lim_{r\to 0}\sqrt{2}r^{-\lambda_1}\sigma_\theta(r,\theta), \mathrm{K}_4 = \lim_{r\to 0}\sqrt{2}r^{-\lambda_1}D_\theta(r,\theta) \tag{23}$$

Here, only GSIFs for θ=0 are investigated.

At first, the effects of mechanical loading τ_z^∞ on the GSIFs are investigated. The GSIFs, $K_3B^{\lambda_1}/\tau_z^\infty$ and $K_4B^{\lambda_1}/\tau_z^\infty$, versus *L/B* are plotted in Figure 4. It is observed that GSIFs are independent of *L/B* as *L/B*>10; The GSIFs for PZT4 inclusion corner tip in PZT5H matrix decrease with increasing of *L/B*, on the contrary, those for PZT5H inclusion corner tip in PZT4 matrix increase with increasing of *L/B*.

On the other hand, the GSIFs, $K_3B^{\lambda_1}$ and $K_4B^{\lambda_1}$, versus *L/B* under electric displacement loading D_y^∞ are plotted in Figure 5. Obviously, the present results of GSIFs are analogous to those under mechanical loading.

5 Conclusions

A new ad hoc hybrid-stress finite element is presented for the antiplane singular electroelastic field analysis of heterogeneous materials with piezoelectric matrix and piezoelectric inclusions. A super *n*-sided polygonal element embedded with a part of an inclusion corner is developed. Versatility and applicability of the developed method are demonstrated by examining the

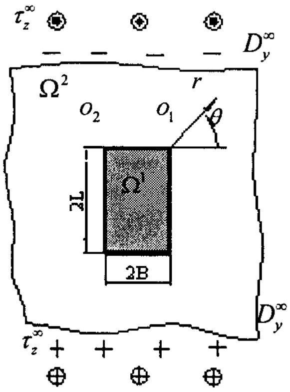

Figure 3: A rectangular inclusion in an infinite matrix

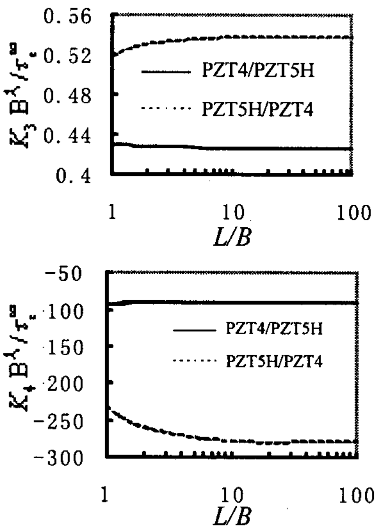

Figure 4: GSIFs versus *L/B* under τ_z^∞

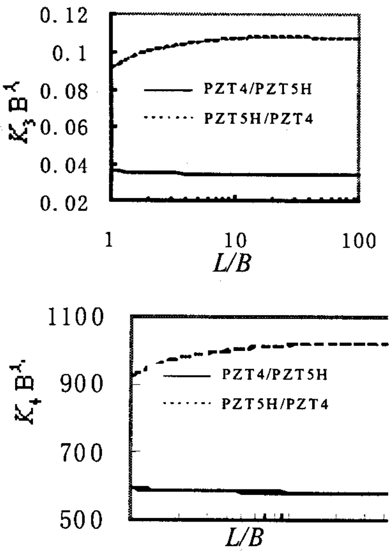

Figure 5: GSIFs versus *L/B* under D^∞

effect of material types and inclusion geometries on the GSIFs of the inclusion corner. In the micromechanics field, the present method seems to have an extensive future.

Acknowledgments

The authors acknowledge the support of National Natural Science Foundation of China through grant No.10362002 and No. 10662004, the Jiangxi Provincial Natural Science Foundation of China through grant No. 2007GZW0862 and the Scientific Research Project of Jiangxi Provincial Department of Education grant NO. GJJ10444.

References

[1] Zhang, T.Y., Tong, P. Fracture Mechanics for a Mode III Crack in a Piezoelectric Material. *International Journal of Solids and Structures*, Vol. 33, p. 343, 1996.
[2] Pak, Y.E., Goloubeva, E. Electroelastic Properties of Cracked Piezoelectric Materials Under Longitudinal Shear. *Mechanics of Material*, Vol. 24, p.287, 1996.
[3] Narita, F., Shindo, Y. Layered Piezoelectric Medium with Interface Crack under Anti-plane Shear. *Theoretical and Applied Fracture Mechanics*, Vol. 30, p. 119, 1998.
[4] Li, X.F., Tang, G.J. Antiplane Interface Crack Between Two Bonded Dissimilar Piezoelectric Layers. *European Journal of Mechanics A/Solids*, Vol. 22,p. 231, 2003.
[5] Qin, Q.H. Solving Anti-plane Problems of Piezoelectric Materials by the Trefftz Finite Element Approach. *Computational Mechanics* Vol. 31, p. 461, 2003.
[6] Chen, M.C., Ping, X.C., Zhu, J.J. Antiplane Singularities Near the Tips of Bonded Piezoelectric-Piezoelectric or Elastic Wedges and Junctions. *Piezoelectricity Acoustic Waves and Device Applications*, World Scientific Publishing Co. Pte. Ltd., Singapore. (in Chinese)
[7] Chue, C.H., Liu, W.J. Antiplane Electro-Mechanical Field of a Piezoelectric Finite Wedge Under Shear Loading and at Fixed-grounded Boundary Conditions. *International Journal of Solids and Structures*, Vol. 44, p. 2540, 2007.
[8] Chen, M.C. Ping, X.C. A Novel Hybrid Finite Element Analysis of Inplane Singular Elastic Field Around Inclusion Corner-tips in Elastic Media. *International Journal of Solids and Structures*, Vol. 46, p.2527, 2009.